Decoding Hand Movement Types and Kinematic Information From Electroencephalogram

Baoguo Xu, Yong Wang, Leying Deng, Changcheng Wu, Wenbing Zhang, Huijun Li, and Aiguo Song, *Senior Member, IEEE*

***Abstract*— Brain-computer interfaces (BCIs) have achieved successful control of assistive devices, e.g. neuroprosthesis or robotic arm. Previous research based on hand movements Electroencephalogram (EEG) has shown limited success in precise and natural control. In this study, we explored the possibilities of decoding movement types and kinematic information for three reach-and-execute actions using movement-related cortical potentials (MRCPs). EEG signals were acquired from 12 healthy subjects during the execution of pinch, palmar and precision disk rotation actions that involved two levels of speeds and forces. In the case of discrimination between hand movement types under each of four different kinematics conditions, we obtained the average peak accuracies of 83.44% and 73.83% for the binary and 3-class classification, respectively. In the case of discrimination between different movement kinematics for each of three actions, the average peak accuracies of 82.9% and 58.2% could be achieved for the two and 4-class scenario. In both cases, peak decoding performance was significantly higher than the subject-specific chance level. We found that hand movement types all could be classified when these actions were executed at four different kinematic parameters. Meanwhile, for each of three hand movements, we decoded movement parameters successfully. Furthermore, the feasibility of decoding hand movements during hand retraction process was also demonstrated. These findings are of great importance for controlling neuroprosthesis or other rehabilitation devices in a fine and natural way, which would drastically increase the acceptance of motor impaired users.**

***Index Terms*— Brain-computer interface, natural hand movement decoding, movement-related cortical potential, kinematic information, EEG.**

Manuscript received May 9, 2021; revised July 22, 2021 and August 18, 2021; accepted August 20, 2021. Date of publication August 24, 2021; date of current version September 2, 2021. This work was supported in part by the Basic Research Project of Leading Technology of Jiangsu Province under Grant BK20192004; in part by the National Natural Science Foundation of China under Grant 61673114, Grant 91648206, and Grant 61803201; and in part by the Fundamental Research Funds for the Central Universities under Grant 3222002102C3. *(Corresponding author: Baoguo Xu.)*

The experimental protocols were approved by the Ethical Committee of Southeast University (2020-SR-362) and each subject gave their informed consent for the study.

Baoguo Xu, Yong Wang, Leying Deng, Wenbing Zhang, Huijun Li, and Aiguo Song are with the State Key Laboratory of Bioelectronics, Jiangsu Key Laboratory of Remote Measurement and Control, School of Instrument Science and Engineering, Southeast University, Nanjing 210096, China (e-mail: xubaoguo@seu.edu.cn; nuaawangyong@163.com; 15695299118@163.com; seuzwb33@163.com; lihuijun@seu.edu.cn; a.g.song@seu.edu.cn).

Changcheng Wu is with the School of Automation Engineering, Nanjing University of Aeronautics and Astronautics, Nanjing 211106, China (e-mail: changchengwu@nuaa.edu.cn).

Digital Object Identifier 10.1109/TNSRE.2021.3106897

I. Introduction

NEUROLOGICAL impairments caused by stroke, spinal cord injury (SCI) and amyotrophic lateral sclerosis (ALS) may lead to the locked-in state [1]. Affected patients will lose their ability to control muscles gradually, although their sensory and cognitive processing often remains largely intact. This situation has a significant effect on the quality of their daily life and their families [2]. Interventions such as surgery and physical therapy are often sought to cushion the resulting effects. When such interventions reach their limits, non-invasive brain-computer interfaces (BCIs) are considered as a promising technical solution in the area of neurological rehabilitation. Utilizing state of art of machine learning algorithms [3]–[6] BCIs can decode brain signals and generate control signals for controlling neuroprosthesis [7], hand rehabilitation robot [8], or a wheelchair [9].

Over the past decades, BCI control strategies have typically relied on repetitive imagination of motor tasks, e.g. hand, foot, and tongue movement. Controlling assistive devices in this way will lead to the inconsistency between the end effector actions and the mental task intentions. It is unnatural for users to imagine the right hand or both feet movement to control the rehabilitation device [10]. Moreover, the fact that the vast majority of existing BCIs usually provide few control signals due to the limited number of imagination tasks, reduces the capability of using these systems to control complicated external devices.

Recently, a new control strategy has attracted researchers' great attention, which focused on the possibility of decoding the hand movements (e.g. palmar, pincer, and lateral grasp) [11]. When we perform different types of hand and finger movements, movement-related cortical potentials (MRCPs) will be elicited in the cerebral cortex during the movement preparation and execution phase [12]–[14]. Some studies reported that similar MRCPs could be observed even by movement imagination/attempt [15], [16]. Typically, MRCPs manifest as a negative shift in amplitude during the process of movement preparation and reach the peak at the onset of movement, followed by a positive rebound in amplitude. It has been shown that features extracted from MRCPs contain sufficient information to decode hand actions [12], [21], upper limb movement [17]–[20], and even movement-related parameters, such as speed and force [22]–[24].

Researchers have been dedicated to discriminating different reach-and-execute actions. Schwarz *et al.* [25] showed that palmar, lateral, and pincer grasps could be classified using

MRCPs in healthy subjects. They also successfully classified unimanual and bimanual reach-and-grasp actions [54]. Ofner *et al*. [26] classified six types of movements of the same upper limb from the low-frequency temporal EEG information. These studies only investigated self-paced movement and did not paid any specific attention to the kinematic information during the execution process of different hand movements. The effect of different motion parameters such as force or speed on the classification performance of natural hand actions is still unclear. Some researchers have paid attention to the kinematics of local joint movements. Jochumsen *et al*. studied the isometric dorsiflexion of right ankle performed at different forces and speeds, and compared different detection and classification methods [23], [27]. Yin *et al*. [28] improved the decoding performance of hand clenching, considering force and speed. However, there are few attempts in decoding the kinematic information of natural arm/hand movements. By distinguishing movement-related parameters of natural hand movements, the possibility of providing a more fine and natural control for the upper-limb neuroprosthesis and other complicated rehabilitation devices could be opened, which is of great significance to the development of natural human-machine interaction system.

We believe that it is promising to investigate natural reach-and-execute actions at two levels of forces and speeds. In this paper, three reach-and-execute movements commonly used in daily life were chosen: (i) pinch grasp, (ii) palmar grasp, (iii) precision disk rotation. The aim of our study was to explore the possibilities of decoding the hand movement types at different speeds or forces and the kinematic information for each of these three actions. Moreover, the hand movement type decoding during execute and release process for three actions was analyzed.

II. Methods

A. Subjects

Twelve right-handed subjects (S1-S12, aged 22-25, six males) participated in the experiment. All subjects were recruited from Southeast University. They were healthy without any known musculoskeletal disorders or neurophysiological anomalies. The experimental protocols were approved by the Ethical Committee of Southeast University (2020-SR-362) and each subject gave their informed consent for the study.

B. Experimental Paradigm

Recording was carried out in a noise-shielded room and subjects were seated in the armchair. An experimental table with a 24-inch screen was placed right in front of them. Three gripping devices designed according to ergonomics were fixed in the fan shape on the experimental table to perform three natural reach-and-execute actions (see Fig. 1 a). Each device included a grip handle and a miniature force sensor to record grasp forces or torque. Note that the two grasp handles and the disk grip handle are all fixed. A pressure button was positioned in the center of this fan-shaped area to ensure that the distances to all three devices were equidistant for each subject. Subjects were instructed to put their right hands on the button. The force produced by the hand movement was used as the input to the system and displayed on the screen where subjects followed the specific force trace we cued.

The maximum force contraction (MFC) for each hand action was determined before the experiment. The average of three maximal force performed was calculated as the reference MFC. Between each contraction there was a rest for 1 min. Subjects were required to perform three natural reach-and-execute actions: pinch grasp, palmar grasp, and precision disk rotation (see Fig. 1 c). For the precision disk rotation, we pay attention to the finger twisting movement of the hand. The specific implementation process is to grasp the fixed disk grip handle and then rotate it with fingers [55]. Each action included four tasks: (i) 3 s to reach 60% MFC, (ii) 0.5 s to reach 60% MFC, (iii) 3 s to reach 20% MFC and (iv) 0.5 s to reach 20% MFC. To assist subjects in performing reach-and-execute actions with the correct force level and the velocity, a cue-based experimental paradigm was adopted, as illustrated in Fig. 2. At second 0, the real-time trace of force appeared on the screen, together with the auditory beep. Subjects were asked to focus on the vertical lines on the screen. After a period of 2.35 s, as the force trace reached the mark position (red vertical line), subjects were instructed to reach toward the specific grip handle. At second 3, subjects performed the natural hand movement at specific level of force and speed, trying to make their force trace match the template trace (see Fig. 2 top). Thereafter, subjects were instructed to release and return their hands to the pressure button. Each trial included a break for 4 s. Subjects were required to keep their face muscle relaxed and avoid blinking or other body movements during the experiment.

We designed 480 trials for three natural reach-and-execute movements with two speeds and two forces. For each condition, 40 repetitions of cued experiments were recorded. Furthermore, we introduced 10 min for break between each session to avoid muscle fatigue. In order to perform the hand movements with various speeds and forces correctly, subjects need to spend 30 min familiarizing our experimental tasks before the formal experiment. The duration of the experiment is ∼4 hours.

C. Signal Acquisition

At the beginning of the experiment, a trigger was generated from Qt software to synchronize EEG record and force data acquisition. To synchronize all trials, event types of different movement-related parameters were sent to EEG amplifier at the beginning of each trial.

Continuous EEG signals were recorded using an active-electrode system (ActiCAP Systems, Brain Products GmbH, Germany) with 64 channels. We selected 40 electrodes positioned over the frontal and parietal lobes (see Fig. 1 b). All channels were referenced to the channel FCz and the electrode FPz was used as the ground when recording. During acquisition, the electrode impedance was kept below 10 KΩ and the sampling frequency was 1000 Hz. To attenuate the high frequency components, we adopted a band-pass Butterworth

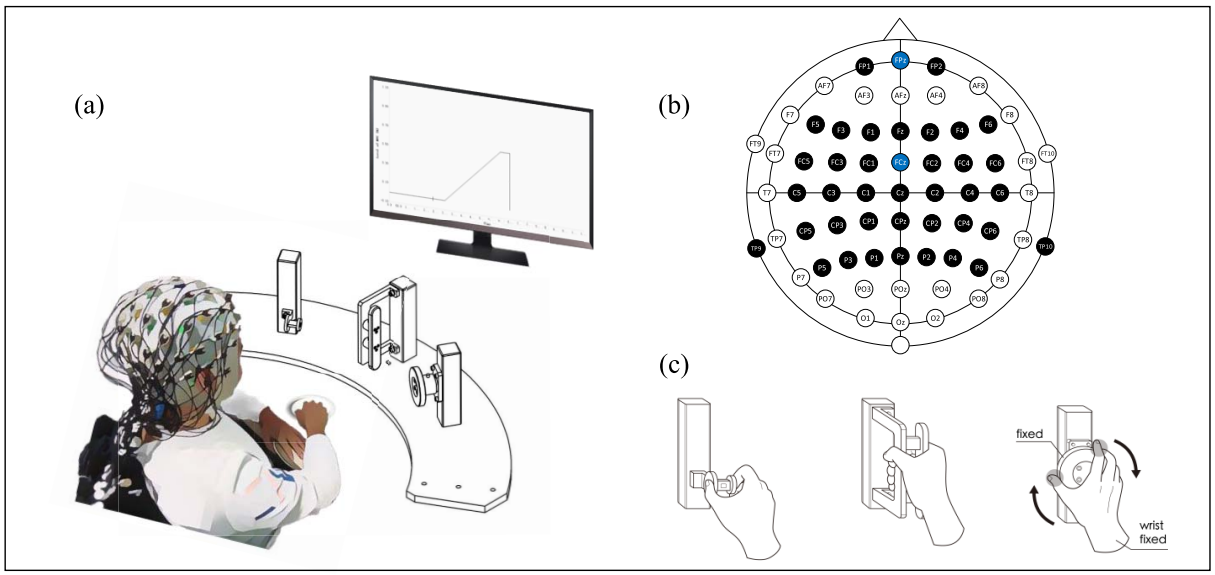

Fig. 1. Experimental setup for three reach-and-execute tasks. a) The experimental table with a screen in front. b) Electrodes set up (black marks). c) Three kinds of hand movements: pinch, palmar and precision disk rotation. For precision disk rotation, subjects preshaped in the type of precision disk grasp [55] and then rotated it with their fingers clockwise instead of their wrists.

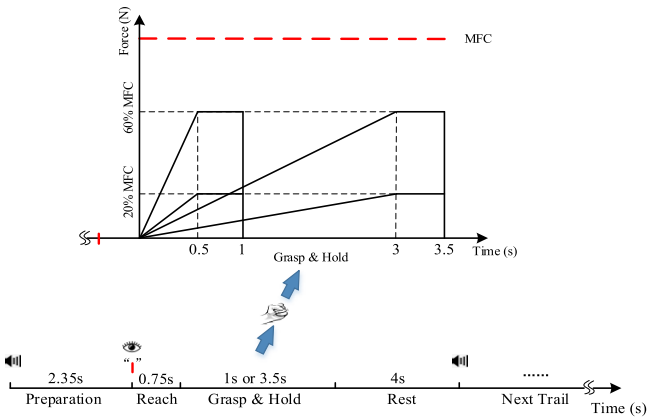

Fig. 2. Experimental paradigm based on the audio and visual cues. At the start of trail, participants put their hands on the pressure button (see Fig. 1 a). Thereafter, they reached out their hands and performed corresponding task, according to the visual cue (Top). Next, participants moved their hand back to the starting position.

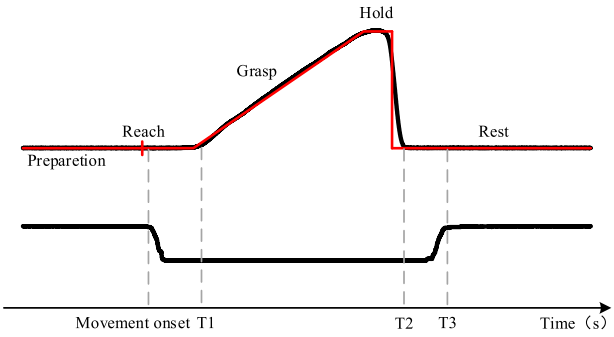

Fig. 3. Detection methods for movement onset and other time points. The red line represents the template of visual cues. Black lines denote the average force (top) and button data (bottom) curve of pinch action for a representative subject.

filter between 0.01 Hz to 100 Hz. In addition, a notch filter at 50 Hz was utilized for the reduction of power line interference.

For natural reach-and-execute movements, forces of pinch and palmar grasps and the torque of precision disk rotation could be recorded using the miniature force transducers on the grip handles. The signals of force data and pressure button (falling edge pulse) were sent to the Qt software using a data acquisition card with six synchronous channels. The signal of force and the button was sampled with 1000 Hz.

D. Movement Time Detection

Fig. 3 presents the representative force trace and the button signal (black line) when the subject matched the visual cue template (red line) during the pinch grasp. In our experiment, the red vertical line on the screen indicated the moment when subjects started to perform the reach-and-execute movements. Due to the individual differences in the reaction time and behavior habits, it could cause significant deviations in the detection of movement onset using this visual cue. Therefore, the falling edge of the pressure button (button release) was detected to determine the movement onset of three reach-and-execute actions for each subject. Movement onset was defined as the average of button release time of each subject. In the similar way, we calculated the finish time of hand retraction (T3) based on the rising edge of the pressure button (button press).

In addition, by analyzing the force trace offline, we also investigated the timings when subjects started their grasps or rotation (T1) and finished their holds (T2). The start time of hand movements (T1) was defined as the initial time when all the force value in the time window of 100 ms exceeded the baseline. The window was shift in step of one sample over each trail and the baseline was calculated as the mean value of button signal during the first interval of 1s of the preparation phase. We detected the time when subjects released the grip handle (T2) in the similar way.

E. Signal Pre-Processing

MRCP has been considered as a low-frequency EEG signal with the low signal-to-noise (SNR) ratio. Before extracting

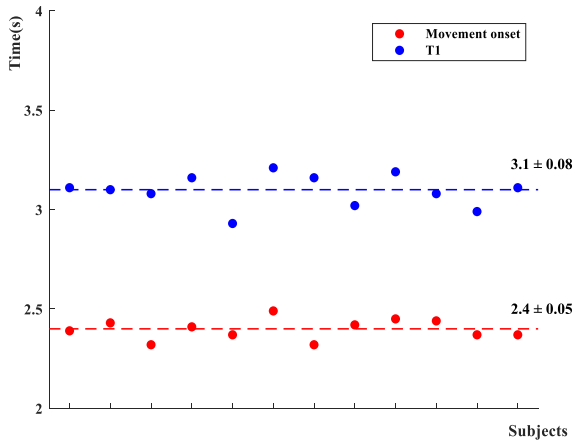

Fig. 4. Behavioral analysis for reach-and-grasp duration. Red dots indicate the movement onset over all subjects. Blue dots represent the time when to perform grasp (T1). Horizon lines represent the average over all subjects for movement onset and T1.

the features for classification, it is necessary to pre-process the raw EEG data. After a low-pass filtering of zero-phase 4th order Butterworth with a cut-off frequency of 45 Hz, all electrodes were re-referenced to the average of the channels TP9 and TP10, which located at mastoids. The discriminative information for movement decoding could be found in the time domain below 6Hz [13]. It is inevitable that frequency range of MRCPs overlaps with electrooculogram (EOG), which leads to the major interference for signal process. Therefore, we adopted independent component analysis (ICA) method to remove the EOG artifacts, utilizing channels FP1 or FP2 as the reference. EEG signals of remaining 35 channels were selected and filtered from 0.03 Hz to 3 Hz using a 4th order zero-phase Butterworth filter to retain its low frequency component. After that, we resampled the signal to 100Hz for the sake of computing performance.

F. Single Trial Classification

MRCPs will be elicited during reach-and-execute movement for three actions. For both the binary and the multiclass classification, we were mainly interested in the two aspects. On the one hand, we tried to decode different actions under each of four kinematic parameters. On the other hand, we wanted to discriminate different kinematic parameters (speed and force) for each of the three actions.

1) Binary Classification: When epoching ours trials with respect to the movement onset, we defined different time regions of interest (tROI) to analyze. Regarding the decoding scheme of action types, we selected the tROI based on period of action execution. For movement type classification at fast speed, the tROI was $[-1, 4]$ s while that of slow speed was $[-1, 6]$ s. With regard to the decoding scheme of motion parameter, the execution time for fast movement (0.5 s) and slow movement (3 s) was different. After 1.5s with respect to movement onset, the hand action was to finish for the fast movement but not for the slow movement. Therefore, the tROI that we chose started 1 s before and ended 1.5 s after movement onset.

For the two aspects, we performed the same feature extraction method based on the pre-processed MRCPs. A 1 s time window sliding every 100 ms was used. We sampled the amplitude values from each of 35 EEG channels in steps of 10ms within this time window. In this way, 35×100 features were obtained and classification model was established every 100ms. For all participants, we divided trials in training sets and testing sets using 5-fold cross-validation procedure. After that, we trained the shrinkage linear discriminant analysis classifier (sLDA) [29] and evaluated its classification performance. Cross validations were repeated 10 times to calculate the grand average accuracy.

2) Multiclass Classification: To estimate the performance of the multiclass classification model, we followed the binary classification procedure. However, following changes were introduced. The multi-class sLDA using "one-versus-one" scheme was adopted instead [30]. In order to improve the computing performance, the steps of taking amplitude values were extended to 100 ms. Furthermore, for kinematic information decoding, the normalized confusion matrices at the specific time point was reported for further analysis. Meanwhile, the multiclass classification performance of twelve subjects were provided in detail.

III. Results

A. Behavior Analysis

In Fig. 4, we show the movement onsets of three actions for each subject, together with timing when subjects started to perform the grasps or rotation (T1). The ultimate movement onset was defined as the average time over all subjects. For three natural hand movements, we analyzed their times together because different actions were cued in the same way and the only difference was the type of action. Moreover, we used the same method to define the time T1. The one-way ANOVA was calculated to check the significant difference of movement onset ($p > 0.88$) and time point T1 ($p > 0.09$) for subjects. Results indicated that the time to reach and the time to execute hand movements had no significant difference for them.

In order to study the entire process of movement, we also report the time when subjects released the grip handle (T2) and when they returned their hands on the button (T3) in Table I. According to our experimental paradigm, movement onset and T1 is consistent for all task conditions, while T2 and T3 will vary for the fast task (0.5 s execution) and the slow task (3 s execution) due to the different speed.

B. Movement-Related Cortical Potentials (MRCPs)

The grand average MRCPs at C1, C2 and Cz channel [11] are shown in Fig. 5. Baseline correction was performed using the mean value in the initial 0.5 s of the preparation phase. Channel C1 and Cz showed relatively higher peak values of MRCPs.

For all action conditions, we could observe an apparent negative shift starting around 1.5 s to 1s before the movement onset. At about 500 ms before the movement onset, a strong and short-term positive rebound oscillating within 3uV could be observed. Furthermore, for each action, the negative shift

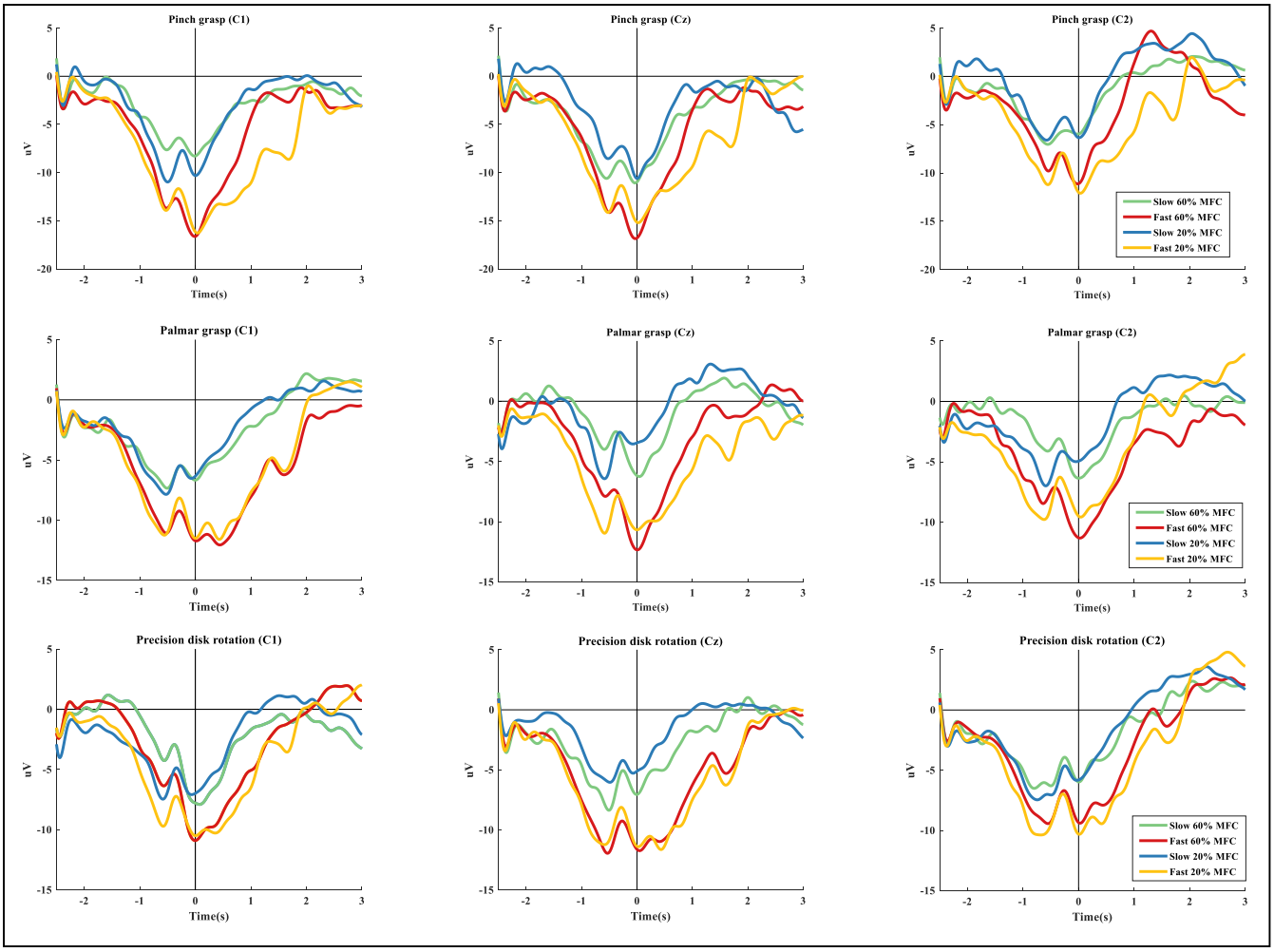

Fig. 5. Grand average of all trails of movement-related cortical potentials (MRCPs) relative to the movement onset for all conditions. 'Fast' means 0.5s to reach the desired level of force and 'slow' means 3 s to reach the same. MRCPs of four different reach-and-execute tasks for three actions were show over channels C1, Cz and C2. Time = 0 s indicates the movement onset.

TABLE I
PHASE TO RELEASE THE GRIP (T2) AND TO RETURN TO THE BUTTON (T3) WITH REGARD TO ACTIONS AT DIFFERENT SPEEDS

Task	T2 (s)	T3(s)
Fast movement	4.08 ± 0.04	4.86±0.23
Slow movement	6.63 ± 0.05	7.41±0.23
	Mean ± STD	**Mean ± STD**

reaches its peak around movement onset. An intermediate positive rebound was observed around 1.5 s after movement onset for those MRCPs produced during fast reach-and-execution movement, which is related to the hand retraction movement. Regarding the negative shift of MRCPs, more pronounced differences can be seen in the movement at different speed than that at different force. The negative rates of the averaged MRCPs were slower for the slow than for the fast hand movements around movement onset ($p < 0.05$). Moreover, different peak amplitudes could be observed between the movements of two speed levels ($p < 0.05$). A similar distinction in peak values could be found between pinch movement and the other two actions

Fig. 6 shows the topographic maps of the pinch grasp of the representative subject under the different kinematic conditions, and the topographic maps during the different force or speed movement are depicted in the time window of [−1s, 1s] with respect to the movement onset. The brain activation was found to change smoothly before the movement onset. We could also observe the differences in the brain activation regions and the degree of the activation under the different kinematic conditions. The difference could be found mainly in the left brain region. Regarding the pinch grasp actions at different speeds, the faster movement could activate more areas of the brain, and to a greater degree, especially around the movement onset. For the pinch grasp at the higher level of MFC, the topographical scalp distribution also showed relatively greater activation.

C. Decoding Hand Movement Types Under Each of Four Kinematic Parameter Conditions

1) Binary Classification Performance: Estimates of binary classification performance across the defined tROI, when combining three action types at different speeds and forces, are shown in Fig. 7. We presented the average results of single trial classification for all subjects with some important time points: movement onset, T1 and T3. For three natural reach-and-execute actions, we reported the whole process of movement execution including hand retraction. Due to our

TABLE II
GRAND-AVERAGE PEAK PERFORMANCE OF BINARY-CLASSIFICATION FOR ACTION PAIRS AND THEIR CORRESPONDING TIME POINT RELATIVE TO THE MOVEMENT ONSET DURING REACH-AND-EXECUTE PHASE

Action pairs	Slow 60% MFC		Fast 60% MFC		Slow 20% MFC		Fast 20% MFC	
	Acc ± STD	Time (s)	Acc ± STD	Time (s)	Acc ± STD	Time (s)	Acc ± STD	Time (s)
Pinch vs Palmar	83.44 ± 9.1	1.0	80.16 ± 6.3	1.0	80.31 ± 8.1	0.8	76.40 ± 9.2	0.9
Pinch vs. Rotation	81.30 ± 9.3	1.0	81.72 ± 6.2	0.9	81.18 ± 5.5	1.0	79.52 ± 5.1	0.9
Palmar vs. Rotation	81.36 ± 6.9	0.9	80.34 ± 7.3	1.1	81.70 ± 6.9	0.9	77.59 ± 7.6	1.0
Average	**82.03** ± 9.0	**1.0**	**80.74** ± 6.8	**1.0**	**81.06** ± 7.1	**0.9**	**77.83** ± 7.7	**0.9**

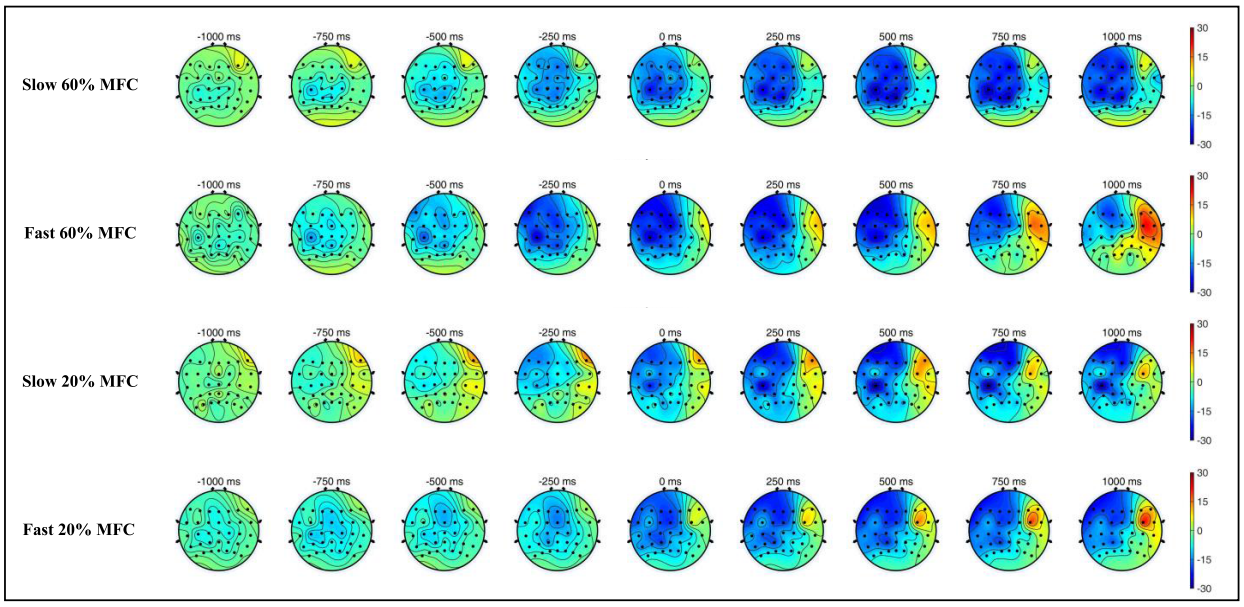

Fig. 6. The time-resolved topographic maps of EEG amplitude of the pinch grasp action during the four different kinematic conditions over the representative subject.

limited number of trials, the chance level is 65.5% (alpha = 0.05, permutation test [31], [32]). Our results show that under the given motion parameters, there is no significant difference between the classification results of the action pairs ($p > 0.05$). For all conditions, peak performance occurred shortly after time point T1. The time when the classification result exceeds the baseline threshold were around t = 0 s. For the slow 20% MFC condition, this time slightly advances by 300ms, while for the fast 20% condition, this time delays 150ms with respect to movement onset.

Table II lists the peak accuracy results of all action combinations as well as its occurrence time with respect to movement onset. Grand average results across motion parameters were included. Action combinations of slow 60% MFC condition achieved grand average peak accuracy of 82.03%. For fast 60% MFC condition and slow 20% MFC condition, the peak results averaged at 80.74% and 81.06% respectively. Considering the worst task condition: fast 20% MFC, peak accuracies of all action pairs were no more that 80%, but nevertheless exceeded the significance threshold of 65.5% by more than 12%. Another peak value of the classification curve in the period of hand retraction was also worthy of our attention. It can be observed that the time for this peak is around 200 ms after the time T3 that corresponds to the end time of hand retraction.

2) Multiclass Classification Performance: Fig. 8 depicts the grand average performance of multiclass classification of action types with the subject-specific chance level lying at 48.1% (alpha = 0.05, permutation test). We show the time region of interest between −1 s and 1.5 s relative to the movement onset. For all conditions of movement-related parameters, better-than-chance classification could be achieved before the movement onset although the performance was limited.

Table III shows the peak accuracy results and true positive rate (TPR) of multiclass classification and the corresponding standard deviation. For the condition of slow 20% MFC, the classification result reaches 73.83% followed by condition of slow 60% MFC (72.5%). In regard to the multi classification for fast 20% MFC, the result of 68.26% is the lowest, but still exceeds the subject-specific chance level by more than 20%. Grand average peak accuracies all occurred about 1s after movement onset.

For each kind of the kinematic condition, we also shows the TPR at the peak time. It can be intuitively observed that all the results could exceed 40% except for the rotation movement under the fast 20% condition. For the highest TPR results, our results even achieved close to 60%.

D. Decoding Four Kinematic Parameters for Each of Three Actions

1) Binary Classification: For kinematic information decoding, the average of the binary classification performance are shown in Fig. 9. The subject-specific chance level was 65.5% (alpha = 0.05, permutation test). Four pairs of task conditions

TABLE III
GRAND-AVERAGE PEAK PERFORMANCE AND TRUE POSITIVE RATE OF ACTION TYPE CLASSIFICATION WITH STANDARD DEVIATION

Condition	Peak Accuracy (%)	True Positive Rate (%)		
		Pinch	Palmar	Rotation
Slow 60% MFC	72.50 ± 17	55.10 ± 1.7	59.83 ± 3.0	56.28 ± 3.8
Fast 60% MFC	71.56 ± 8.1	45.14 ± 5.4	46.34 ± 4.4	48.09 ± 2.1
Slow 20% MFC	73.83 ± 5.7	46.67 ± 1.7	53.90 ± 3.5	52.27 ± 4.1
Fast 20% MFC	68.26 ± 11	43.90 ± 4.7	44.34 ± 6.4	41.46 ± 2.4
	Mean ± STD	**Mean ± STD**	**Mean ± STD**	**Mean ± STD**

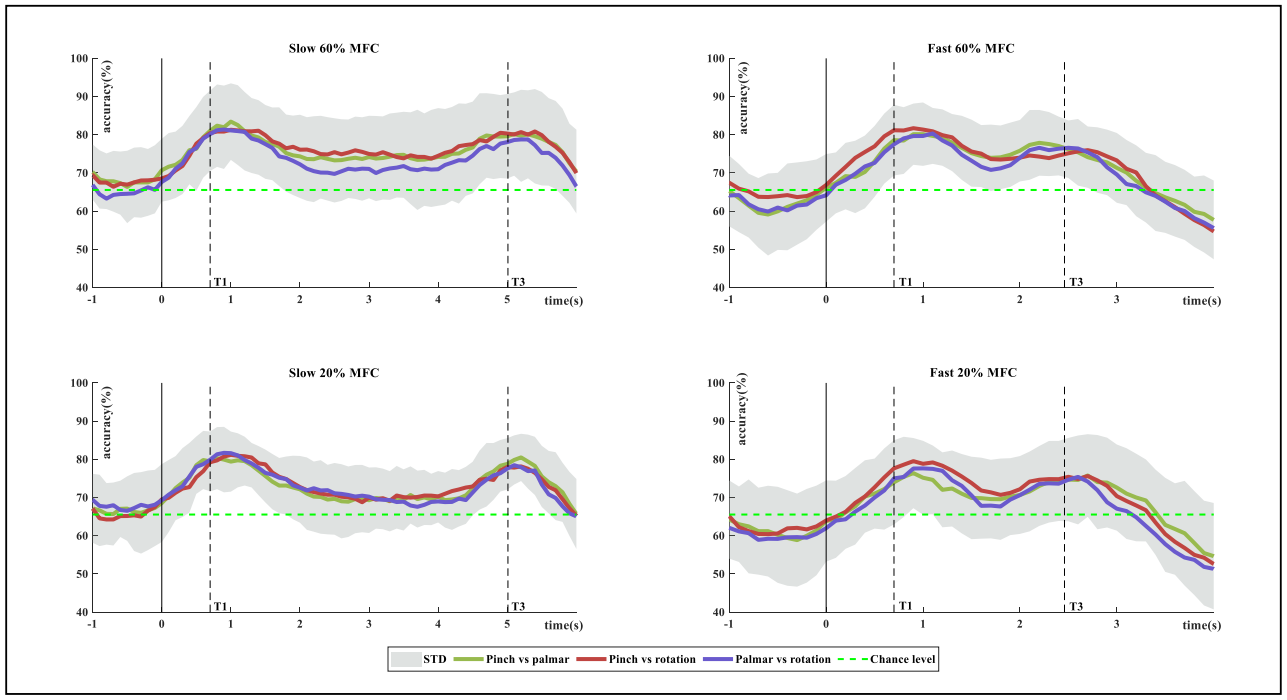

Fig. 7. Binary classification results of action pairs for different motion parameters relative to movement onset. Grand average of classification accuracies with standard deviation are plotted. The black perpendicular solid line at second 0 marks the movement onset, and the dotted line marks the time T1 and T3 respectively.

classified over the tROI of [−1, 1.5] s were (i) slow 60% MFC vs slow 20% MFC, (ii) fast 60% MFC vs fast 20% MFC, (iii) slow 60% MFC vs fast 60% MFC and (iv) slow 20% MFC vs fast 20% MFC.

In most conditions, the classification results can exceed the chance level before the movement onset. However, for precision disk rotation, the classification performance is relatively poor and a delay in the time for exceeding the chance level can be observed relative to movement onset, especially for condition of fast 60% MFC versus fast 20% MFC (∼500 ms). Even so, the peak accuracy of its decoding performance still exceeds the baseline.

Table IV presents the peak classification accuracy of movement-related parameter for each of three actions. Moreover, grand average results across motion parameter pairs and the occurrence time of the peak results relative to movement onset was shown. During the period of tROI, it can be observed that all task pairs achieve its peak accuracy about 1s after the movement onset. For each natural hand movement, we achieved the peak accuracies higher than 70%.

Table V demonstrates the precision results of binary classification of the kinematic parameter pairs for each of three actions. For slow 60% MFC versus fast 60% MFC, the highest precision could reach 86.14% (pinch grasp) and the averaged

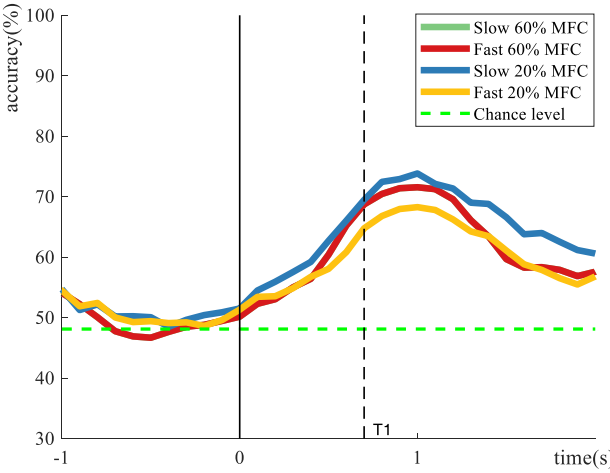

Fig. 8. Grand average multiclass classification results of action types over all subjects under different motion parameters.

results was 82.26%. For fast 60% MFC versus fast 20% MFC, the precision results averaged at 74%.

2) Multiclass Classification: For each of three different natural reach-and-execute actions, we investigated the multi-classification performance of kinematic parameters as illustrated in Fig. 10 (top left). Peak accuracy culminates at

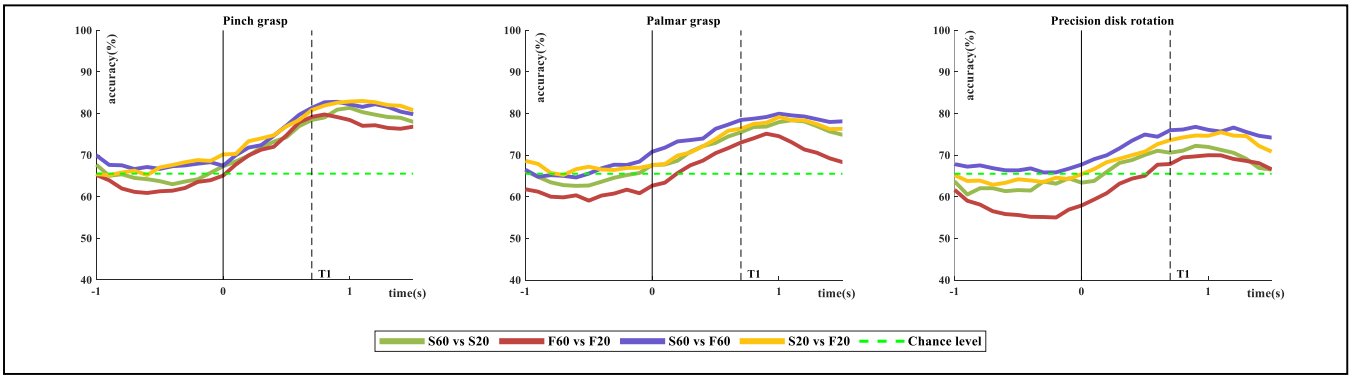

Fig. 9. Grand average binary classification results of different kinematic parameter pairs over all subjects. The black perpendicular solid line at second 0 marks the movement onset, and the dotted line marks the time T1. S60: Slow 60% MFC, S20: Slow 20% MFC, F60: Fast 60% MFC, F20: Fast 20% MFC.

TABLE IV

GRAND AVERAGE PEAK PERFORMANCE OF BINARY-CLASSIFACATION FOR DIFFERENT PAIRS OF KINEMATIC PARAMETERS AND THEIR CORRESPONDING TIME POINT RELATIVE TO THE MOVEMENT ONSET

Action types	S60 versus F60		F60 versus F20		S60 versus F60		S20 versus F60	
	Acc ± STD (%)	Time (s)	Acc ± STD (%)	Time (s)	Acc ± STD (%)	Time (s)	Acc ± STD (%)	Time (s)
Pinch	81.38 ± 8.9	1.0	79.78 ± 9.2	0.8	82.82 ± 7.9	0.9	82.90 ± 5.0	1.0
Palmar	78.41 ± 7.6	1.1	75.18 ± 9.1	0.9	79.98 ± 8.2	1.0	79.17 ± 6.1	1.0
Rotation	72.26 ± 5.9	0.9	70.01 ± 8.0	1.0	76.82 ± 5.8	0.9	75.52 ± 7.2	1.1
Average	**77.35 ± 9.3**	**1.0**	**74.99 ± 9.1**	**0.9**	**79.87 ± 8.2**	**0.9**	**79.20 ± 6.9**	**1.0**

TABLE V

THE PRESICINO OF BINARY-CLASSIFACATION FOR DIFFERENT PAIRS OF KINEMATIC PARAMETERS AND THEIR CORRESPONDING TIME POINT RELATIVE TO THE MOVEMENT ONSET

Action types	S60 versus F60		F60 versus F20		S60 versus F60		S20 versus F60	
	Precision (%)	Time (s)	Precision (%)	Time (s)	Precision (%)	Time (s)	Precision (%)	Time (s)
Pinch	82.04 ± 11	1.0	78.58 ± 12	0.8	86.14 ± 9	0.9	84.49 ± 11	1.0
Palmar	81.41 ± 12	1.1	75.59 ± 8	0.9	82.10 ± 10	1.0	81.52 ± 10	1.0
Rotation	77.09 ± 11	0.9	70.02 ± 10	1.0	81.53 ± 11	0.9	77.98 ± 12	1.1

58.2% (pinch grasp), 57.84% (palmar grasp) and 51.28% (precision disk rotation), which all exceed the chance level of 38.2 % (alpha = 0.05, permutation test). Higher classification performance can be observed in pinch and palmar grasp condition. For palmar action, a better-than-chance result could be achieved up to 500ms before movement onset while the time is ∼300ms for pinch and rotation actions. For all hand movements, their peak time occur around 1s after movement onset.

In Fig. 10 (bottom), we demonstrated the row normalized confusion matrixes at the time point of peak accuracy for each hand movement. The true positive rates for different movement parameter conditions all exceeded the values of 40%. However, the false positive rates could reach 30.23% for precision disk rotation movement. Moreover, we presents subject-specific results at the peak time in Fig. 10 (top right). It is worth mentioning that the classification of movement parameters of subject 6 could get the accuracy higher than 70% for each of hand movements.

IV. DISCUSSION

In this paper, we investigated decoding performance relative to movement types and kinematic information for three natural reach-and-execute actions.

Our results successfully classified movement types under each of four different kinematic conditions. Binary classification result of 83.44% for action versus action condition was achieved. For multiclass classification, the accuracy of 73.83% could be attained.

Furthermore, we demonstrated that it was possible to discriminate four movement-related parameters for each of three reach-and-execute actions. In the binary decoding scenario, classification performance for motion parameters versus motion parameters condition peaked at 82.9%. With regard to multiclass decoding scenario, the highest results of classification accuracy could reach 58.2%.

A. Movement-Related Cortical Potentials

MRCPs is often shown to be elicited during self-initiated movement paradigm [15]. Consistent with the MRCPs described by Jochumsen in [23], the amplitudes manifested the negative shift as early as 1.5s before the movement onset and reach its maximum around the movement onset (t = 0s). In our study, we found a weak positive potential rebound before the movement onset (Fig. 5). Furthermore, negative peaks of pinch grasp were higher than other two actions. In addition, peak negative shifts of the C1 and Cz electrodes are more pronounced than that of the C2 electrode for the contralateral control of the brain. This phenomenon indicates that the natural movement of the right hand will activate the left-brain area more, as illustrated in Fig. 7. Shibasaki *et al.* [33] revealed that the MRCPs potential contains sufficient decoding information, including speed and force parameters. Analysis of MRCPs

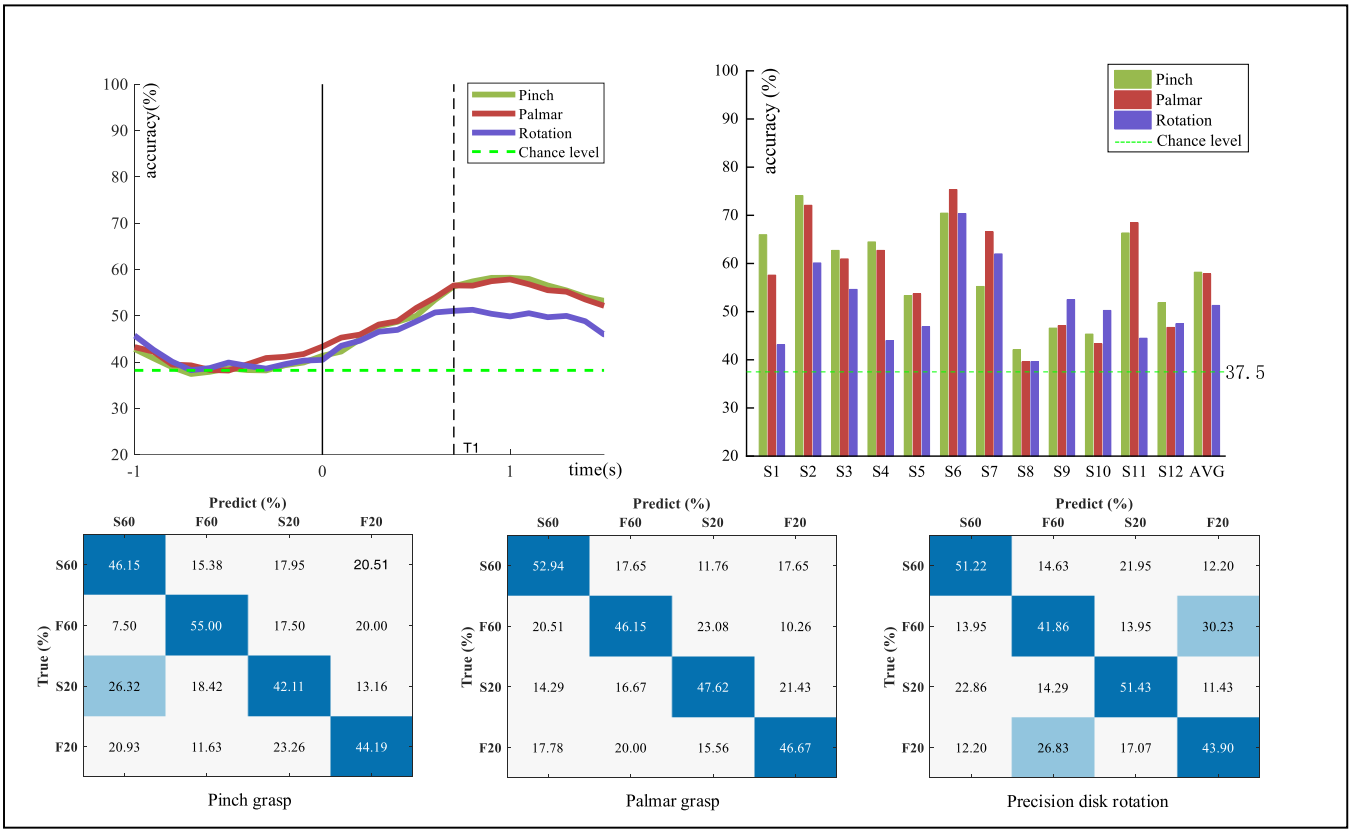

Fig. 10. Multiclass classification results of motion parameters for each of three actions. Top left plots the grand-average decoding accuracies over all subjects. Top right shows the subject-specific accuracies at the time of grand average peak performance. The green dashed lines represent the significant threshold. Bottom shows confusion matrixes normalized by row at the peak time for three actions.

produced by the same action showed that the difference in potentials generated by actions at different speed is more pronounced than actions at different force. Gu *et al*. [34] found the greater rebound rate of MRCPs for faster wrist movement than for slow wrist movement. The similar results could be found for each of three natural actions in our study.

For the time-resolved topographical maps of pinch grasp under different kinematic conditions, the degree of brain activation for each kind of movement increased before the movement onset smoothly, and decreased gradually, as the execution of the action came to the end. From the comparison of topographical map in the 1s period before and after movement onset, we could conclude that the faster or more forceful movement helps to activate more areas of the brain and to a deeper degree. Additionally, in terms of brain regions activated, most of them were located in the left-brain region. These results were consistent with our above analysis.

B. Movement Time Detection

In this study, pressure button and miniature force sensors were used to record the time points during movement execution. The calculation results showed that the standard deviation of T0 and T1 were below 100ms, while the standard deviation of T3 reached 230ms. Although we adopted the similar calculation method, due to influence of factors such as visual cues and personal habits, standard deviations of T0, T1 and T3 were different.

C. Single Trial Classification

The theoretical chance level of the binary classification should be 50%. In the three-class and four-class task, this value is supposed to be 33% and 25%, respectively. The actual threshold could exceed these levels for the limited number of trials. In this research, we comprehensively considered the experimental time and the fatigue of subjects. Each movement related task contains 40 trials to ensure the performance of task execution. The significant thresholds of different cases were adjusted and the peak classification accuracies of two aspects that we focused on were obtained.

1) Decoding Hand Movement Types Under Each of Four Kinematic Parameter Conditions: Single trial binary classification for action versus action conditions attained high classification results ranged from 76.40% to 83.44%. Schwarz *et al.* [35] reached an averaged peak accuracy of 75% for binary classification (rest vs palmar vs lateral) using combined features. Direct comparison may be difficult because the experimental setup and actions of the research were not exactly the same. It should be noted that four different movement parameter conditions were considered to classify different hand actions in this study. We found that action pairs could be successfully classified under each of these kinematic conditions. Additionally, it can be observed from Fig. 7 that the classification performances for action pairs in the condition of fast 20% MFC are all below the chance level at movement onset. Meanwhile, for condition of slow 60% MFC, the average peak result of the action pairs reached highest, which yielded

4.2% higher than that of fast 20% MFC condition. Analyzing the decoding performance at different speed or force, we can conclude that slower and more forceful execution is beneficial for movement discrimination between different actions.

For the multiclass classification of action types, we achieved the highest classification accuracy of 73.83%. Ofner *et al.* [26] decoded six different upper limb movements and indicated that discrimination between movements including different joints are significantly better than the grasps. Different with their work, three kind of hand movements that did not include wrist rotation were investigated in this study. As can be seen in Table III, multiclass classification at slow 20% MFC and slow 60% MFC shows a slightly better performance than that at the other two conditions. The poorest performance was observed for the condition of fast 20% MFC. It is reasonable to believe that greater force or speed can induce more discrimination information between actions. Moreover, from our results, the parameter of speed seems to have a greater impact on the classification performance of hand movement types. Yuan *et al*. [36], [37] demonstrated the possibility of decoding the speed of imagined hand movement and analyzed the spectral-temporal dynamics systematically.

2) Decoding Four Kinematic Parameters for Each of Three Actions: For three natural hand movements, we combined four pairs of movement-related tasks. Peak accuracies were obtained during the execution phase and all exceeded the subject-specific chance level. Movements at different speeds will cause inconsistent of execution time. For the fast movement, subjects were instructed to complete the grasp or rotation action around the time point of 1.5s after movement onset, while the action execution process continued for the slow movement. Therefore, the time of interest for kinematic classification performance was defined in the time range between −1s to 1.5s relative to the movement onset (see Fig. 9). In our experiments, the accuracy of single-trial binary classification could reach 82.9% for pinch grasp. In line with the study of [11], the time of peak classification of our study is bout 1000ms with respect to movement onset, which delays by ∼300ms compared to the time when the force starts to be applied. In addition, consistent with study of [23], the parameter classification results (accuracies and precisions) of different speeds show better performance than that of different forces but does not depend on the action types. Regarding different actions, our investigations reveal that pinch movement obtains better discrimination performance than palmar and rotation movement when trying to distinguish different speeds and forces.

The results from multiclass classification of different movement parameters show that peak accuracy of 58.2% could be obtained around 1s after movement onset. It is notable that precision disk rotation action achieves a peak accuracy of 51.28%, which is lower than results of the other two actions. It is believed that the differences in the way of hand movement execution may be the potential reason. Jochumsen *et al.* [22] studied the isometric palmar grasps and classified single-trial movement execution associated with two levels of force and speed, with the accuracy result of 41% ± 7% (4 class). With respect to the limit classification accuracy of their study, we scored a significantly higher result for each of three hand actions.

Regarding the confusion matrix, it could be observed that the performance of multiclass decoding is biased. For pinch grasp, the highest values on the diagonal was fast 60% MFC condition. For palmar and rotation actions, slow 60% MFC and slow 20% MFC condition got the highest values. Nevertheless, for each hand movement, the TPRs of four movement-related parameters all exceeded the chance level of 38.2% and differed by no more than 15%. In addition, the experiment recruited twelve subjects and subject 8 showed poor movement parameters classification results for each of the three actions, but still exceeded the significant threshold. With respect to the best classification performance of subject 6, the decoding accuracy were higher than 70% for each of three actions.

D. Hand Retraction

For the hand retraction process in Fig. 9, the discrimination performance is observed, which is an unexpected and interesting discovery. Binary classification of various natural actions yields high average result ranging from 75.61% to 79.94%. The peak time delays no more than 300ms related to T3. For each subject, this time may be advanced or delayed because of the high standard deviation of the time T3 (200ms). Compared with the classification performance of action pairs in the reaching and holding phase, the average classification result is slightly lower in the process of hand retraction. Nevertheless, exceeding chance level by more than 10% means that it is feasible to decode the movement of hand retraction after the task execution. The intermediate positive rebounds of different actions during the hand retraction process in MRCPs showed the underlying neural differences (see Fig. 5). This phenomenon is expected because the inverse process of the natural reach-and-execute movement should also contain specific motion information for decoding. Unfortunately, there are few researches in this area for us to compare.

E. Limitations and Future Work

In this study, we investigated three types of natural hand movement: pinch, palmar and precision disk rotation. Our results indicated that it is feasible to decoding action types regardless of the kinematics. For each of three different hand movements, the kinematic information could be decoded utilizing MRCPs. Previous BCI studies have shown success in robotic arm control for hand movement tasks and relied on motor imagination (MI) [38]–[40]. However, classifying natural actions based on MRCPs can be much more natural and responsive to the user's subjective feelings than MI tasks. In addition, the EEG-based control of robotic arms is mostly discrete or staged, and the kinematic parameters of the end-effector (speed of tension and strength of grasp, etc.) are fixed or pre-designed [40], [41]. For many daily-life scenarios, the subjective and flexible control of the force or speed for hand movements are required, such as grasping objects of different weights and hardness, grasping objects that are fragile or deformable, and rotating different objects.

Schwarz *et al.* [42] have shown successful online decoding of the lateral grasp, palmar grasp and wrist supination movement, and implemented the manipulation of the robotic arm in a simulated environment. Compared with their rough control, our research could introduce more flexibility and precision for control strategy. Although our analysis was performed offline, further research on our basis can improve the performance of brain-actuated robotic arm or prosthesis, especially for the complex operation tasks.

To assist participants in the precise control on the speed and force during action execution, we adopted a cued-based experiment protocol, which was different with the self-initiated movement in MRCPs [43]. Additionally, our study was not carried out on the SCI patients and the command strategy was generated by the execution of the movement, which makes it a challenge to transfer our results to actual end users decline due to the distinctions in the muscle control ability between the patients and healthy subjects. Ofner *et al.* [44] have shown a similar neural representation for decoding between the executed movement and the attempted movement. Blokland *et al.* [45], [46] indicated that the movement attempt may be more suitable for command strategy than the movement imagination. We also envision a possible future solution where the residual function of end users could be utilized to the maximum extent, such as performing the reaching movement followed by the non-functional hand attempted movement. A further study on the user group with motor impairment is necessary to evaluate our results, although it is challenging.

It is notable that the extracted features in our study are based on time domain only. The intricate and non-stationary properties of EEG make it a challenge to improve the decoding performance. Researchers have shown that discriminable information for decoding precision and power hand movements could be found over higher frequency bands, especially for alpha band [47], [48]. For three self-paced movements of rest, palmar and lateral grasp, study of [35] have shown that the classification performance of sLDA classifier could be improved by 10% by combining the spectral power values of α and β bands, compared with the simple time-domain features. Therefore, further studies are possible to consider the combination of frequency and time-domain features. Although the simplicity and efficiency of the classifier make it easier for online implementation, the performance of classification model in our study is still need to be further evaluated. Some of the latest models in the motor imagination (MI) paradigm could brought us inspiration. Deep learning algorithms can not only be used for extract various features from time-frequency images or EEG source imaging, but also for EEG analysis to boost the decoding performance [49]–[51]. Lee *et al.* [52] has showed that the proposed end-to-end convolutional neural network (CNN) could perform well on the 3-class, 5-class and 7-class classification tasks for nine different arm MI movements. Recent study has shown the ability of CNN structure to learn a wide variety of interpretable features over a range of BCI tasks, including the MRCP-based paradigm [53]. In the future work, it is reasonable to combine hybrid features with the deep learning techniques to boost the decoding performance.

V. Conclusion

This study investigated three natural reach-and-execute actions performed at two levels of speeds and forces. On the one hand, we demonstrated that three movement types can be successfully decoded under each of four different movement-related parameter conditions. On the other hand, it was found that four different kinematic parameters could be discriminated better than chance level for each of three natural actions. Based on the analysis of whole process of natural movements, we also presented the feasibility of decoding different movement types during the hand retraction process, which is the inverse process of the natural reach-and-execute movement.

Investigations on natural actions with kinematic information are of great importance for the application in the BCI system. We believe that despite the issues such as transferring to end users and online experiment, which still needs to be further addressed, our works can make potential contributions to the fine and natural control of rehabilitation robot, especially for neural prosthesis.

References

[1] A. Kübler, B. Kotchoubey, J. Kaiser, J. R. Wolpaw, and N. Birbaumer, "Brain–computer communication: Unlocking the locked in," *Psychol. Bull.*, vol. 127, no. 3, pp. 358–375, 2001.

[2] A. Moss *et al.*, "Patients with amyotrophic lateral sclerosis receiving long-term mechanical ventilation. Advance care planning and outcomes," *Chest*, vol. 110, no. 1, pp. 249–255, 1996.

[3] F. Lotte *et al.*, "A review of classification algorithms for EEG-based brain-computer interfaces: A 10 year update," *J. Neural Eng.*, vol. 15, no. 3, p. 31005, 2018.

[4] N. Jiang, L. Gizzi, N. Mrachacz-Kersting, K. Dremstrup, and D. Farina, "A brain–computer interface for single-trial detection of gait initiation from movement related cortical potentials," *Clin. Neurophysiol.*, vol. 126, no. 1, pp. 154–159, Jan. 2015.

[5] A. Hyvärinen, "Fast and robust fixed-point algorithms for independent component analysis," *IEEE Trans. Neural Netw.*, vol. 10, no. 3, pp. 626–634, May 1999.

[6] C. Lin, B. Wang, N. Jiang, R. Xu, N. Mrachaczkersting, and D. Farina, "Discriminative manifold learning based detection of movement-related cortical potentials," *IEEE Trans. Neural Syst. Rehabil. Eng.*, vol. 24, no. 9, pp. 921–927, Sep. 2016.

[7] G. R. Müller-Putz, R. Scherer, G. Pfurtscheller, and R. Rupp, "Brain-computer interfaces for control of neuroprostheses: From synchronous to asynchronous mode of operation," *Biomed. Tech.*, vol. 51, no. 2, pp. 57–63, 2006.

[8] Y. He, D. Eguren, J. M. Azorín, R. G. Grossman, T. P. Luu, and J. L. Contreras-Vidal, "Brain-machine interfaces for controlling lower-limb powered robotic systems," *J. Neural Eng.*, vol. 15, no. 2, p. 21004, 2018.

[9] F. Galan *et al.*, "A brain-actuated wheelchair: Asynchronous and non-invasive brain-computer interfaces for continuous control of robots," *Clin. Neurophysiol.*, vol. 119, pp. 2159–2169, Sep. 2008.

[10] G. Pfurtscheller, C. Guger, G. Müller, G. Krausz, and C. Neuper, "Brain oscillations control hand orthosis in a tetraplegic," *Neurosci. Lett.*, vol. 292, no. 3, pp. 211–214, 2000.

[11] A. Schwarz, P. Ofner, J. Pereira, A. I. Sburlea, and G. R. Müller-Putz, "Decoding natural reach-and-grasp actions from human EEG," *J. Neural Eng.*, vol. 15, no. 1, p. 16005, 2018.

[12] H. Shibasaki and M. Hallett, "What is the bereitschaftspotential?" *Clin. Neurophysiol.*, vol. 117, no. 11, pp. 2341–2356, 2006.

[13] T. Pistohl, A. Schulze-Bonhage, A. Aertsen, C. Mehring, and T. Ball, "Decoding natural grasp types from human ECoG," *NeuroImage*, vol. 59, no. 1, pp. 248–260, 2012.

[14] S. M. Slobounov and W. J. Ray, "Movement-related potentials with reference to isometric force output in discrete and repetitive tasks," *Exp. Brain Res.*, vol. 123, no. 4, pp. 461–473, Nov. 1998.

[15] J.-H. Jeong, N.-S. Kwak, C. Guan, and S.-W. Lee, "Decoding movement-related cortical potentials based on subject-dependent and section-wise spectral filtering," *IEEE Trans. Neural Syst. Rehabil. Eng.*, vol. 28, no. 3, pp. 687–698, Mar. 2020.

[16] N. Birbaumer, T. Elbert, A. G. Canavan, and B. Rockstroh, "Slow potentials of the cerebral cortex and behavior," *Physiological Rev.*, vol. 70, no. 1, pp. 1–41, Jan. 1990.

[17] J.-H. Jeong, K.-H. Shim, D.-J. Kim, and S.-W. Lee, "Trajectory decoding of arm reaching movement imageries for brain-controlled robot arm system," in *Proc. 41st Annu. Int. Conf. IEEE Eng. Med. Biol. Soc. (EMBC)*, Jul. 2019, pp. 5544–5547.

[18] A. Úbeda, J. M. Azorín, R. Chavarriaga, and J. D. R. Millán, "Classification of upper limb center-out reaching tasks by means of EEG-based continuous decoding techniques," *J. Neuroeng. Rehabil.*, vol. 14, no. 1, pp. 1–14, Dec. 2017.

[19] J.-H. Jeong, K.-T. Kim, D.-J. Kim, and S.-W. Lee, "Decoding of multi-directional reaching movements for EEG-based robot arm control," in *Proc. IEEE Int. Conf. Syst., Man, Cybern. (SMC)*, Oct. 2018, pp. 511–514.

[20] M. Jochumsen *et al.*, "Quantification of movement-related eeg correlates associated with motor training: A study on movement-related cortical potentials and sensorimotor rhythms," *Frontiers Hum. Neurosci.*, vol. 11, p. 604, Dec. 2017.

[21] P. Ahmadian, S. Sanei, L. Ascari, L. Gonzalez-Villanueva, and M. A. Umilta, "Constrained blind source extraction of readiness potentials from EEG," *IEEE Trans. Neural Syst. Rehabil. Eng.*, vol. 21, no. 4, pp. 567–575, Jul. 2013.

[22] M. Jochumsen, C. Rovsing, H. Rovsing, I. K. Niazi, K. Dremstrup, and E. N. Kamavuako, "Classification of hand grasp kinetics and types using movement-related cortical potentials and EEG rhythms," *Comput. Intell. Neurosci.*, vol. 2017, Aug. 2017, Art. no. 7470864.

[23] M. Jochumsen, I. K. Niazi, N. Mrachacz-Kersting, D. Farina, and K. Dremstrup, "Detection and classification of movement-related cortical potentials associated with task force and speed," *J. Neural Eng.*, vol. 10, no. 5, p. 56015, 2013.

[24] D. Farina, O. F. D. Nascimento, M.-F. Lucas, and C. Doncarli, "Optimization of wavelets for classification of movement-related cortical potentials generated by variation of force-related parameters," *J. Neurosci. Methods*, vol. 162, nos. 1–2, pp. 357–363, May 2007.

[25] A. Schwarz, C. Escolano, L. Montesano, and G. R. Müller-Putz, "Analyzing and decoding natural Reach-and-Grasp actions using gel, water and dry EEG systems," *Frontiers Neurosci.*, vol. 14, p. 849, Aug. 2020.

[26] P. Ofner, A. Schwarz, J. Pereira, and G. R. Müller-Putz, "Upper limb movements can be decoded from the time-domain of low-frequency EEG," *PLoS ONE*, vol. 12, no. 8, Aug. 2017, Art. no. e0182578.

[27] M. Jochumsen, I. K. Niazi, N. Mrachacz-Kersting, N. Jiang, D. Farina, and K. Dremstrup, "Comparison of spatial filters and features for the detection and classification of movement-related cortical potentials in healthy individuals and stroke patients," *J. Neural Eng.*, vol. 12, no. 5, p. 56003, 2015.

[28] X. Yin *et al.*, "A hybrid BCI based on EEG and fNIRS signals improves the performance of decoding motor imagery of both force and speed of hand clenching," *J. Neural Eng.*, vol. 12, no. 3, p. 36004, 2015.

[29] B. Blankertz, S. Lemm, M. Treder, S. Haufe, and K.-R. Müller, "Single-trial analysis and classification of ERP components—A tutorial," *NeuroImage*, vol. 56, no. 2, pp. 814–825, May 2011.

[30] R. O. Duda, P. E. Hart, D. G. Stork, and R. O. P. C. A. S. A. Duda, *Pattern Classification*, 2nd ed. New York, NY, USA: Wiley, 2001.

[31] G. Müller-Putz, R. Scherer, C. Brunner, R. Leeb, and G. Pfurtscheller, "Better than random: A closer look on BCI results," *Int. J. Bioelectromagn.*, vol. 10, no. 1, pp. 52–55, 2008.

[32] E. Combrisson and K. Jerbi, "Exceeding chance level by chance: The caveat of theoretical chance levels in brain signal classification and statistical assessment of decoding accuracy," *J. Neurosci. Methods*, vol. 250, pp. 126–136, Jul. 2015.

[33] H. Shibasaki, G. Barrett, E. Halliday, and A. M. Halliday, "Cortical potentials associated with voluntary foot movement in man," *Electroencephalogr. Clin. Neurophysiol.*, vol. 52, no. 6, pp. 507–516, Dec. 1981.

[34] Y. Gu, K. Dremstrup, and D. Farina, "Single-trial discrimination of type and speed of wrist movements from EEG recordings," *Clin. Neurophysiol.*, vol. 120, no. 8, pp. 1596–1600, Aug. 2009.

[35] A. Schwarz, J. Pereira, L. Lindner, and G. R. Müller-Putz, "Combining frequency and time-domain EEG features for classification of self-paced reach-and-grasp actions," in *Proc. 41st Annu. Int. Conf. IEEE Eng. Med. Biol. Soc. (EMBC)*, Jul. 2019, pp. 3036–3041.

[36] H. Yuan, C. Perdoni, and B. He, "Relationship between speed and EEG activity during imagined and executed hand movements," *J. Neural Eng.*, vol. 7, no. 2, p. 26001, 2010.

[37] H. Yuan, C. Perdoni, and B. He, "Decoding speed of imagined hand movement from EEG," in *Proc. Annu. Int. Conf. IEEE Eng. Med. Biol.*, Aug. 2010, pp. 142–145.

[38] Y. Xu *et al.*, "Shared control of a robotic arm using non-invasive brain–computer interface and computer vision guidance," *Robot. Auto. Syst.*, vol. 115, pp. 121–129, May 2019.

[39] D. Suma, J. Meng, B. J. Edelman, and B. He, "Spatial-temporal aspects of continuous EEG-based neurorobotic control," *J. Neural Eng.*, vol. 17, no. 6, Dec. 2020, Art. no. 066006.

[40] J. Meng, S. Zhang, A. Bekyo, J. Olsoe, B. Baxter, and B. He, "Non-invasive electroencephalogram based control of a robotic arm for reach and grasp tasks," *Sci. Rep.*, vol. 6, no. 1, pp. 1–15, Dec. 2016.

[41] X. Han, K. Lin, S. Gao, and X. Gao, "A novel system of SSVEP-based human-robot coordination," *J. Neural Eng.*, vol. 16, no. 1, p. 16006. 2018.

[42] A. Schwarz, M. K. Höller, J. Pereira, P. Ofner, and G. R. Müller-Putz, "Decoding hand movements from human EEG to control a robotic arm in a simulation environment," *J. Neural Eng.*, vol. 17, no. 3, p. 36010, 2020.

[43] M.-K. Lu, N. Arai, C.-H. Tsai, and U. Ziemann, "Movement related cortical potentials of cued versus self-initiated movements: Double dissociated modulation by dorsal premotor cortex versus supplementary motor area rTMS," *Hum. Brain Mapping*, vol. 33, no. 4, pp. 824–839, 2012.

[44] P. Ofner, A. Schwarz, J. Pereira, D. Wyss, R. Wildburger, and G. R. Müller-Putz, "Attempted arm and hand movements can be decoded from low-frequency EEG from persons with spinal cord injury," *Sci. Rep.*, vol. 9, no. 1, pp. 1–15, Dec. 2019.

[45] Y. Blokland *et al.*, "Detection of attempted movement from the EEG during neuromuscular block: Proof of principle study in awake volunteers," *Sci. Rep.*, vol. 5, no. 1, pp. 1–10, Oct. 2015.

[46] Y. Blokland *et al.*, "Detection of event-related desynchronization during attempted and imagined movements in tetraplegics for brain switch control," in *Proc. Annu. Int. Conf. IEEE Eng. Med. Biol. Soc.*, Aug. 2012, pp. 3967–3969.

[47] I. Iturrate *et al.*, "Human EEG reveals distinct neural correlates of power and precision grasping types," *NeuroImage*, vol. 181, pp. 635–644, Nov. 2018.

[48] P. Fries, "Rhythms for cognition: Communication through coherence," *Neuron*, vol. 88, no. 1, pp. 220–235, Oct. 2015.

[49] B. Xu *et al.*, "Wavelet transform time-frequency image and convolutional network-based motor imagery EEG classification," *IEEE Access*, vol. 7, pp. 6084–6093, 2018.

[50] Y. Hou, L. Zhou, S. Jia, and X. Lun, "A novel approach of decoding EEG four-class motor imagery tasks via scout ESI and CNN," *J. Neural Eng.*, vol. 17, no. 1, p. 16048, 2020.

[51] A. Craik, Y. He, and J. L. Contreras-Vidal, "Deep learning for electroencephalogram (EEG) classification tasks: A review," *J. Neural Eng.*, vol. 16, no. 3, p. 31001, 2019.

[52] B.-H. Lee, J.-H. Jeong, K.-H. Shim, and S.-W. Lee, "Classification of high-dimensional motor imagery tasks based on an end-to-end role assigned convolutional neural network," in *Proc. IEEE Int. Conf. Acoust., Speech Signal Process. (ICASSP)*, May 2020, pp. 1359–1363.

[53] V. Lawhern, A. Solon, R. Waytowich, M. Gordon, P. Hung, and B. Lance, "EEGNet: A compact convolutional neural network for EEG-based brain-computer interfaces," *J. Neural Eng.*, vol. 15, no. 5, p. 56013, 2018.

[54] A. Schwarz, J. Pereira, R. Kobler, and G. R. Muller-Putz, "Unimanual and bimanual reach-and-grasp actions can be decoded from human EEG," *IEEE Trans. Biomed. Eng.*, vol. 67, no. 6, pp. 1684–1695, Jun. 2020.

[55] T. Feix, J. Romero, H. Schmiedmayer, A. M. Dollar, and D. Kragic, "The GRASP taxonomy of human grasp types," *IEEE Trans. Hum.-Mach. Syst.*, vol. 46, no. 1, pp. 66–77, Feb. 2016.